

A torsional balance for the characterization of microNewton thrusters

Manuel Gamero-Castaño^{a)}

Busek Co. Inc., 11 Tech Circle, Natick, Massachusetts 01760

(Received 25 April 2003; accepted 11 July 2003)

We describe the performance of a torsional balance suitable for the study of microNewton thrusters. A design based on flexural pivots and electrostatic forces (for calibration and active damping) makes it possible to test thrusters with a mass of a few kilograms, and measure submicroNewton level forces with high accuracy and a resolution better than $0.03 \mu\text{N}$. The usefulness of the balance is proved by measuring the performance of two different electric propulsion accelerators: a colloid thruster generating thrust in the $2\text{--}13 \mu\text{N}$ range, and a micropulsed plasma thruster yielding single impulse bits of $19 \mu\text{N s}$. The low noise figure of the balance (below $0.1 \mu\text{N}/\sqrt{\text{Hz}}$ in the $7 \text{ mHz--}1 \text{ Hz}$ bandwidth) will make it possible to measure the thrust noise requirements imposed in colloid thrusters by missions such as the Space Technology 7 and the Laser Interferometer Space Antenna.

© 2003 American Institute of Physics. [DOI: 10.1063/1.1611614]

I. INTRODUCTION

In addition to the expected proliferation of nano- and microsatellites, ongoing scientific missions, such as NASA's Space Technology 7 (ST7),¹ and NASA and ESA's Laser Interferometer Space Antenna (LISA),² need propulsion at the microNewton level to achieve their mission goals. The propulsion requirements can be stringent. For example, the NASA ST7 mission calls for thrusters capable of delivering thrust along the $2\text{--}20 \mu\text{N}$ range, with a resolution of $0.1 \mu\text{N}$, and a noise figure better than $0.1 \mu\text{N}/\sqrt{\text{Hz}}$ in the $1\text{--}100 \text{ mHz}$ bandwidth. Furthermore, the thrusters must operate continuously.

Devices of the type of micro pulsed plasma thrusters (microPPTs)³ and solid propellant microthrusters⁴ are being developed to fill this propulsion niche. Field emission electric propulsion⁵ and colloid thrusters⁶ are generally recognized as the two existing technologies that can match the exceptional requirements imposed by missions like ST7 or LISA. The development of these technologies depends on the characterization of their propulsive properties; in particular, measuring the thrust with the required precision is paramount. Although diagnostic tools such as the time of flight technique can be used to measure thrust in some cases, it is apparent that a force balance, or thrust stand, is a more universal and direct solution, and hence the preferred apparatus.

The first thrust stand able to resolve forces of a few microNewtons appears to be the early work by Stark *et al.*⁷ Their "micropound extended range thrust stand," based on flexural pivots and electromagnetic forces for calibration and damping, was used to measure both continuous and impulsive thrust. Several designs with higher resolution and sometimes operating in the submicroNewton range have recently appeared in the literature.^{4,8,9} The work by Ziemer deserves special mention because of its quality and characterization of different thrusters.¹⁰ A variety of technical hurdles handicaps the design and operation of microNewton thrust stands: the

weight of the thruster can be as large as a few kilograms, and matching structural strength and measuring sensitivity is difficult; the inherently "noisy" environment surrounding the balance can completely overwhelm its motion; accurate calibration at this low force level is an additional problem; and, in some cases, the natural dynamics of the balance have to be compensated to obtain a more tractable response.

In this article we present a torsional balance specially designed to test micropropulsion thrusters. It can support weights of up to 44 kg, and measure forces with a resolution better than $0.03 \mu\text{N}$. Its accuracy is limited only by the precision with which linear distances and voltages can be measured. The article is organized as follows: after Sec. I we will describe the main features of the torsional balance. Section III presents measurements of the "continuous" thrust produced by a colloid thruster. The capability of the balance for measuring impulse bits is exemplified in Sec. IV using a microPPT. All the results presented in this article were taken under actual experimental conditions, which included work in vacuum (provided by a 250 l/s turbomolecular pump and a 13.8 cfm belt-drive mechanical pump) while supporting a thruster (typically 0.5 kg) and a counterweight.

II. BALANCE DESCRIPTION

Figure 1 shows a schematic of the torsional balance. An aluminum frame fixed to the vacuum facility supports the swinging arm. The inclination of the frame is adjusted with two stepper motors. The arm rotates around the axis defined by two aligned flexural pivots (Lucas Aerospace, Utica, N.Y.) attached to both the frame and the arm. Each pivot can support an axial load of up to 431 N. The linear displacement of the arm at 0.220 m from the axis of rotation is measured with a fiber optic linear displacement sensor (LDS) (Philtec, Arnold, MD). Its nominal resolution is 5.0 nm in the dc–100 Hz range, dropping to $0.15 \mu\text{m}$ at a frequency of 200 kHz. The relation between the output of the sensor (the signal in volts reported in some of the following figures) and the optical gap was calibrated *in situ* with a $10 \mu\text{m}$ resolution mi-

^{a)}Electronic mail: mgamero@busek.com

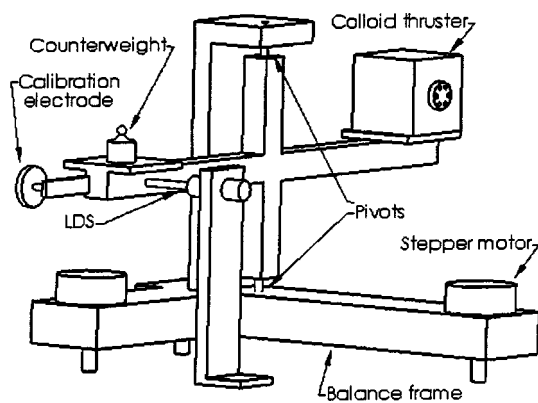
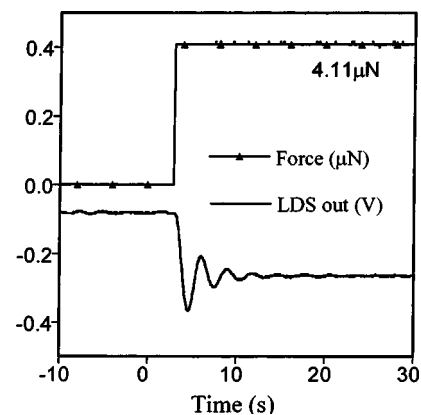


FIG. 1. Schematics of the torsional balance.

FIG. 2. Balance's response to a $1.09 \mu\text{Nm}$ torque excitation.

rometer. Typically, the nominal value of the gap was 0.1 mm, well within the range of linear operation of the sensor. Its calibration value is $8.03 \mu\text{m/V}$.

A set of electrodes (two facing disks) was used to calibrate the balance displacement resulting from a given torque. One disk was attached to the balance and had a diameter of 5.08 cm, while the second disk was fixed to an external positioner and had a diameter of 1.90 cm; the gap between the disks, L , was typically 1.10 mm (the actual value was measured for each calibration). The distance between the axis of the disks and the axis of the balance was 0.266 m. An electrostatic force is a good option to excite the balance because: (a) it acts at a distance, i.e., there is no physical contact between the rotating arm and the forcing element; (b) the electrostatic force can be accurately computed; (c) its amplitude can be varied "continuously," and (d) its time variation can be controlled in scales much smaller than that of the characteristic response time of the balance. The electrostatic force, F , on the surface of the electrodes was computed using the software packages MAXWELL 2D and MAXWELL 3D, versions 9 (the two dimensional and three dimensional calculations converged within 0.5%). The calculated values are well fitted by the formula

$$\frac{F}{V^2} = 1.262 \times 10^{-9} \frac{1}{L^2} (1 + 138.1 \times L),$$

in $\mu\text{N/V}^2$, L expressed in meters, (1)

where V is the voltage difference between the electrodes. Note that, for a 1 mm gap, the calculated force is 13.8% larger than the estimate derived from the assumption of a homogeneous electric field between the electrodes. The difference is due to the excess charge on the edges existing in the real electrode geometry, which is accurately captured by the Laplace's equation solver. We have used the calibration in Eq. (1) to compute all the force measurements in this article. We also used electrostatic forces between an additional set of electrodes to implement an active linear damper and reduce the oscillatory nature of the balance's motion. An analog circuit controller commanded the damper.

The dynamics of the torsional balance are well described by the harmonic oscillator equation

$$i \ddot{\vartheta} + \lambda \dot{\vartheta} + \kappa \vartheta = L(t), \quad (2)$$

where ϑ is the rotation angle of the arm, i is its moment of inertia about the axis of rotation, and λ and κ are damping and torsional spring rate constants. $L(t)$ is the torque applied to the balance, which can be a function of time. Figure 2 illustrates how the balance responds to a torque applied with the calibration electrodes. A step force of $4.11 \mu\text{N}$ (torque of $1.09 \mu\text{Nm}$) is exerted and the resulting motion of the balance is monitored. Note that the noise to signal ratio of the balance output is quite small at this microNewton level. Repeating this measurement with different excitation levels, a static calibration of the balance is computed. Such a calibration is shown in Fig. 3, where all four axes are used to display the relevant parameters (calibration force and torque, LDS output in Volts, and displacement measured by the LDS). The relation between the LDS output, and the exciting torque is quite linear and has a negligible interception with the y axis, which makes it possible to compute the torsional spring rate accurately. We get $\kappa = 0.0192 \mu\text{N/mV}$, or written in the physical units of Eq. (2), $\kappa = 0.140 \text{ N m/rad} = 0.00244 \text{ N m/deg}$ (the relation between LDS output and displacement is $8.03 \mu\text{m/V}$; the distance between LDS and the axis of rotation is 0.220 m; the lever arm of the calibration electrode is 0.266 m).

The magnitude of the sinusoidal transfer function of the balance, $\|G(f)\|$, is shown in Fig. 4. The frequency response was obtained with a colloid thruster weighing 0.450 kg and

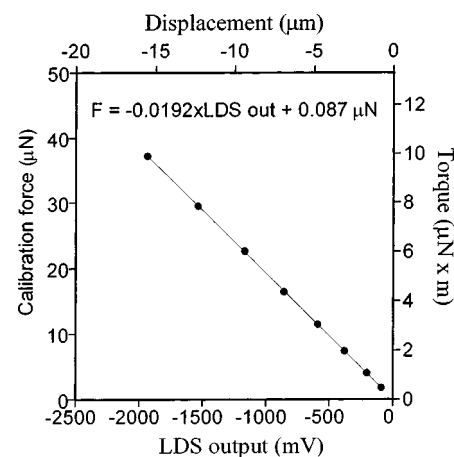


FIG. 3. Balance's steady state calibration.

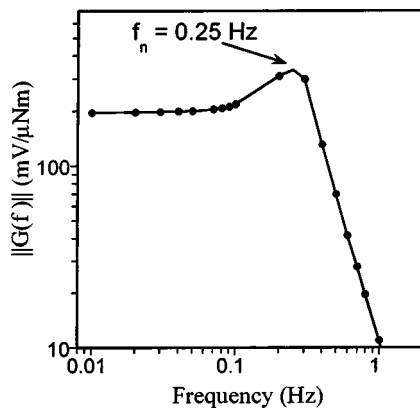


FIG. 4. Balance's frequency response.

an identical counterweight placed on the balance, which increased its moment of inertia and hence its natural period. A sinusoidal torque at varying frequencies was applied with the calibration electrodes. The transfer function in Fig. 4 is the product of the transfer functions of the second order system associated with the balance dynamics, and that of an analog, first order *RC* filter used to condition the output of the LDS. The resulting response resembles a low pass filter with a cut off frequency around 0.4 Hz. The natural frequency of the balance can be estimated from the resonance peak in Fig. 4, $f_n \sim 0.25$ Hz.

III. MEASURING "CONTINUOUS" THRUST: COLLOID THRUSTERS

Colloid thrusters are electrostatic accelerators of charged electro spray droplets.^{6,11} They generate thrust continuously in the microNewton range, with a low thrust noise and ample throttleability. These capabilities are essential for drag-free missions such as the New Millennium Program's ST7, which is designed to maintain a spacecraft's position with respect to a free-floating test mass to less than $10 \text{ nm}/\sqrt{\text{Hz}}$, over the frequency range 1–30 mHz.¹² In fact, colloid thrusters are one of two technologies, gravity sensors being the second one, on which the ST7 mission is based. We have used the torsional balance to measure the thrust generated by a six-emitter colloid thruster. The electro spray source was mounted inside a grounded aluminum box, which also contained a reservoir filled with propellant (see Fig. 1 for a sketch of the thruster). Thin copper wires connected the electrodes of the electro spray source to two external high voltage power supplies. These connections were designed to make spurious torques on the balance, induced by the electrostatic and tensile forces associated with the wires, negligible. The lever arm of the thruster was 0.254 m. A typical measurement session is illustrated in Fig. 5. We plot the signals associated with the emitter voltage, V_n , the electro spray beam current, I_n , and the balance output, T , as a function of time. The measuring procedure is as follows: the electro spray source is initially in operation ($V_n = 2.07 \text{ kV}$, $I_n = 2.75 \mu\text{A}$), yielding a thrust of $7.89 \mu\text{N}$. The offset of the balance signal is determined by turning off the power connected to the electro spray source (see voltage and current curves at $t \sim 46 \text{ s}$), which causes the balance signal to relax

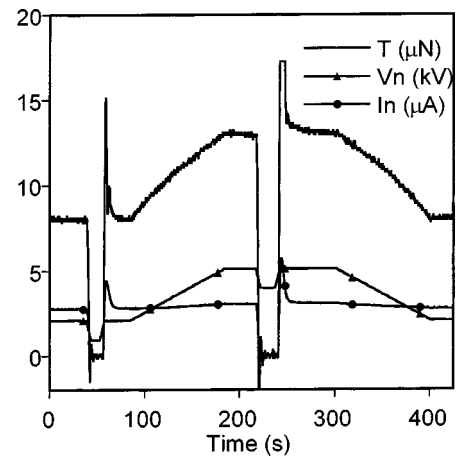


FIG. 5. Typical thrust measurements with a colloid thruster.

to its equilibrium position. Once the equilibrium position is determined, the electro spray source is turned back on. It takes a few second for the thrust to reach its steady state value because the extra amount of propellant surrounding the emitters, accumulated during the power off period, needs to be fully extracted. The acceleration voltage is then ramped up, which results in an increase of the thrust, until a value of 5.07 kV ($12.9 \mu\text{N}$) is reached. The equilibrium position of the balance is determined again by shutting down the electro spray source, and finally the acceleration voltage is ramped down to the initial value of 2.07 kV. This experimental run was taken at constant propellant mass flow rate (i.e., roughly constant beam current). We have repeated this procedure at different flow rates and mapped the thrust versus beam current versus acceleration voltage surface in the 2.33–12.9 μN , 1.34–2.75 μA , and 2.07–5.07 kV domain.¹³

After demonstrating throttleability and quasicontinuous thrust variation, we will analyze the power spectrum of the balance output. We aim to find the lower limit beyond which the noise of the colloid thruster cannot be directly characterized by the balance (the noise figure is the most stringent requirement imposed on the thruster performance by missions like ST7). Figure 6 shows a recording of the balance output during 10 000 s at a sampling rate of 0.2 s. Both calibration electrodes and colloid thruster are off; i.e., this spectrum reflects the free motion of the balance in the ab-

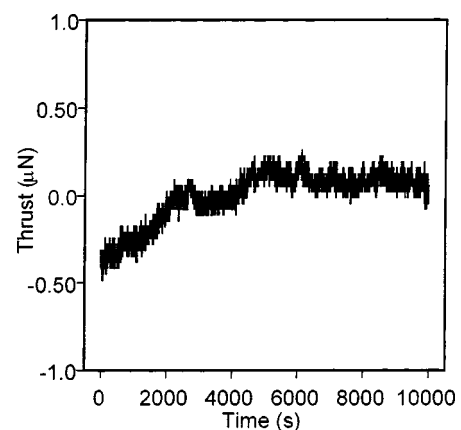


FIG. 6. Recording of the intrinsic motion of the balance during 10 000 s.

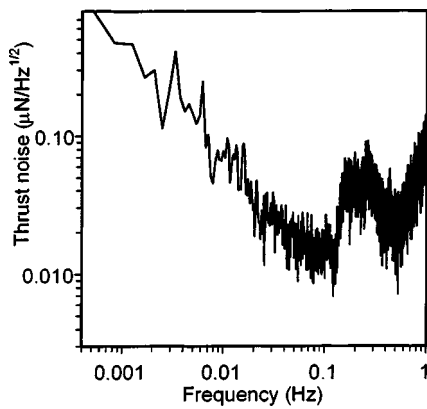


FIG. 7. Power spectrum density per unit time of the data in Fig. 6.

sence of intentionally applied torques. The thrust scale is referred to the position of the colloid thruster (lever arm of 0.254 m). An interesting feature of these data is the small variation of the balance offset, especially in the interval between 5000 and 10000 s. We can estimate the balance resolution by computing the standard deviation of these data. To do so, we divided the data into 20 s windows (this stretch, made of five natural periods of the balance-colloid thruster system, contains enough points to obtain a representative average of the balance output), computed the standard deviation of each window, and averaged the standard deviations. We obtain an averaged standard deviation of $0.034 \mu\text{N}$. Note that this is a conservative estimate for the resolution, because at this 20 s scale most of the signal variation is actually due to oscillations of the balance at frequency values around 0.25 Hz (the energy transmitted to the balance by spurious sources of external noise is mostly dissipated by oscillations at the balance's natural frequency), and the effect of these oscillations on the measurement is greatly reduced by averaging the signal during five natural periods of the balance. A second relevant figure of the balance performance is its offset drift rate. The average of the values for each 20 s window is 0.80 nN/s , and thus the averaged drift of the balance during a 20 s period is $0.016 \mu\text{N}$.

The noise spectrum of the 10000 s series, Fig. 6, is shown in Fig. 7. The time span of this series makes it possible to compute the power spectrum down to the low frequencies of interest for the ST7 mission. We have used the following standard procedures to compute the spectrum: it is based on the power spectrum density per unit time of the thrust; in order to reduce the variance of the periodogram estimation, the original series of sampled points was partitioned into four segments, and we averaged the square root of the power spectra at every discrete frequency; and the linear trend was subtracted from each data window. Returning to Fig. 7, note that the noise spectrum of the balance is approximately $0.02 \mu\text{N}/\sqrt{\text{Hz}}$ at 0.1 Hz, and monotonically increases for lower frequencies, reaching the value of $0.1 \mu\text{N}/\sqrt{\text{Hz}}$ at 7 mHz. We expect to improve this figure by reducing external noise sources, and thus positively test the $0.1 \mu\text{N}/\sqrt{\text{Hz}}$ constraint imposed by the ST7 mission on colloid thrusters along the required bandwidth, (1, 100 mHz). The spectrum in Fig. 7 also shows how the noise peaks

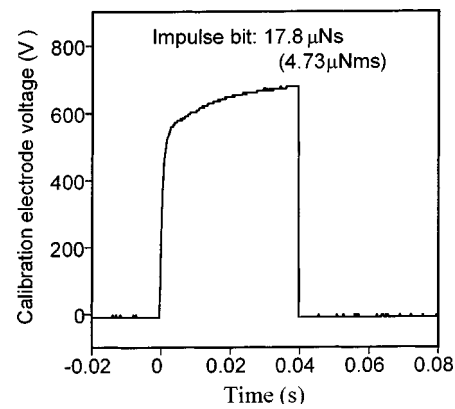


FIG. 8. Impulsive excitation of the balance using calibration electrodes.

around the natural frequency of the balance, $f_n \sim 0.25 \text{ Hz}$. The noise increase at still larger frequencies is irrelevant to our application, and it is likely due to poor filtering of electrical noise typical of higher frequencies, which is aliased into the bandwidth of Fig. 7. The aliasing is amplified above 0.25 Hz by the steep decline of the balance's transfer function (see Fig. 4).

IV. THRUST IMPULSE BIT MEASUREMENT: MICRO PULSED PLASMA THRUSTER

The total momentum generated by a pulsed plasma thruster can be accurately measured with a torsional balance. This thruster operates through brief plasma discharges (typically they last a few microseconds), each of them transferring a given momentum, or thrust impulse bit, and which repeated at a given frequency translate into an averaged thrust. Because, during each shot, the interaction forces between the exhaust plasma and the thruster occur in an instant, t_d , several orders of magnitude smaller than the natural period of the balance, t_n , the motion of the latter cannot follow instantaneously the exciting force. But, because the momentum is conserved, the impulse bit associated with the discharge can be accurately modeled by an initial condition on the balance velocity. Thus, the response of the balance to an impulsive force is described by Eq. (2) with the right-hand side equal to zero, and with initial conditions $\vartheta(0)=0$ and $\dot{\vartheta}(0)=P/I$, where P is the time integral of the impulsive force (or, more correctly, the impulsive torque) associated with the discharge

$$P = \int_0^{t_d} L(t) dt, \quad t_d \ll t_n. \quad (3)$$

Thus, as long as the characteristic time of the discharge is much smaller than the characteristic response time of the balance, the motion of the balance, $\vartheta(t)$, is strictly a function of the total momentum transferred by the discharge, P , and does not depend on the particular shape of $L(t)$. Using this fact, together with our electrostatic calibration forces, we will show in the following paragraphs how to obtain an accurate calibration between thrust impulse bit and the balance signal. In these experiments the balance was holding a microPPT¹⁴ weighing 0.652 kg and an identical counterweight in the opposite side; the lever arm of the microPPT

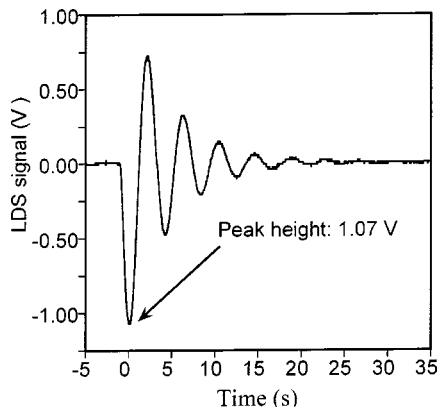


FIG. 9. Balance's response to the impulse bit in Fig. 8.

was 0.174 m; and the lever arm of the calibration electrode was, as in the colloid thruster experiments, 0.266 m.

First, it is easy to prove that the solution for $\vartheta(t)$ is proportional to P , and in particular, the height of the first oscillation peak resulting from the impulsive excitation is also proportional to P . Second, because $\vartheta(t)$ is independent of the exact shape of $L(t)$ for a given P , we can use the "arbitrarily fast acting" electrostatic force to obtain the desired calibration. The methodology is illustrated in Figs. 8, 9, and 10. Figure 8 plots the voltage difference between the electrodes while simulating an impulsive force. The interaction lasted 40 ms, 100 times shorter than the natural period of the balance; it has a pulse-like shape topping 677 V, and the associated momentum is $17.8 \mu\text{N s}$ (or $4.73 \mu\text{N m s}$). The motion of the balance caused by this pulse is shown in Fig. 9. Note that the electrostatic damper eliminated the oscillations after a few cycles. The height of the first peak, h , as given by the electronics of the LDS, is 1.07 V. This process can be repeated several times, resulting in the P versus h calibration shown in Fig. 10, which collects impulse bit values in the range $3.45\text{--}39.3 \mu\text{N s}$, with excitation intervals between 20 and 80 ms. Note that, as in the case of the static calibration shown in Fig. 3, this calibration exhibits a good linearity and a small interception of the linear fitting with the ordinate axis, which supports the quality of the actual thrust measurements.

Figure 11 shows the response of the balance to a single shot of the microPPT. The signal named "discharge voltage"

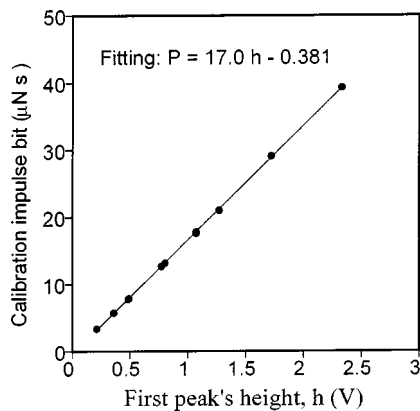


FIG. 10. Impulse bit calibration of the balance.

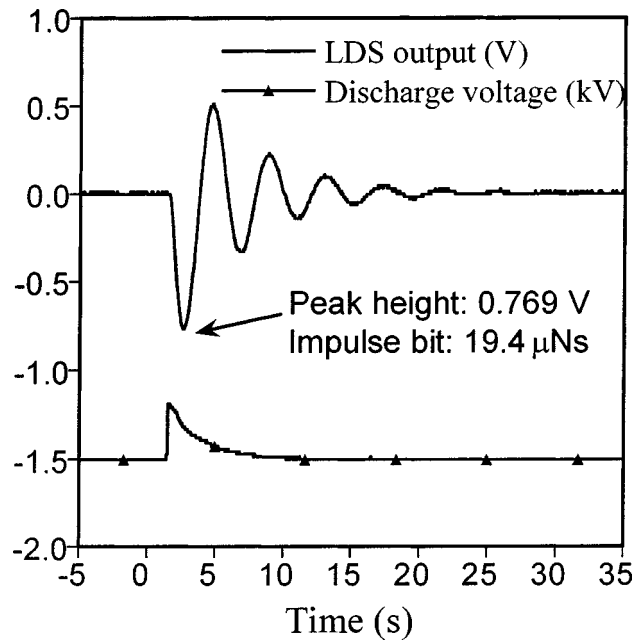


FIG. 11. Balance's motion induced by a single microPPT shot.

was a mere indication of when the microPPT is triggered. Naturally, the evolution of the signal is similar to that shown in Fig. 9, since the impulsive nature of the excitation was the same in both cases. The height of the first oscillation peak is 0.769 V, and hence the total momentum associated with the discharge is $19.4 \mu\text{N s}$ (the lever arm of the μPPT is 0.174 m; the lever arm of the calibration electrodes is 0.266 m). The discharge voltage was 1460 V, and the energy stored in the capacitors previous to the discharge was 2.1 J. Finally, Fig. 12 shows the impulse bits of 20 single shots, all of them having the discharge parameters of the previous case. The balance measurements indicate that the microPPT discharges are quite repeatable, at least from the point of view of momentum transfer to the thruster.

ACKNOWLEDGMENTS

The construction of the torsional balance was funded by NASA SBIR contract no. NAS3-00017. Additional research work was funded by the Jet Propulsion Lab and the U.S. Air

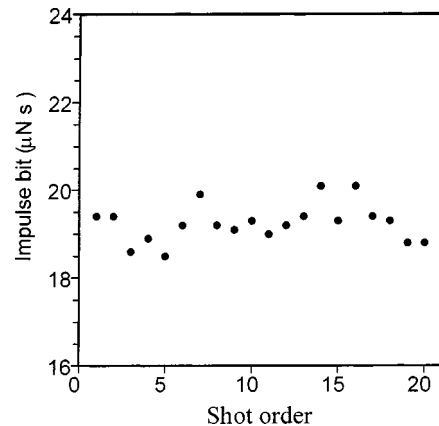


FIG. 12. Collection of microPPT impulse bits for a nominal set of discharge conditions.

Force Research Laboratory. The authors greatly acknowledge the support given by the technical monitors of these programs, J. Sovey (NASA), W. Folkner and G. Man (JPL), and D. Bromaghim (AFRL). They also acknowledge the help of Professor M. Martínez-Sánchez (M.I.T.) and V. Hruby (Busek), both of whom are responsible for the original mechanical design of the balance.

- ¹W. Folkner, G. Keiser, S. Buchman, R. L. Byer, V. Hruby, and M. Gamero-Castaño, *Proc. SPIE* **4860** (2002); G. Keiser, S. Buchman, R. L. Byer, W. Folkner, V. Hruby, and M. Gamero-Castaño, *ibid.* **4856** (2002).
²T. T. Hyde and P. G. Maghami, American Astronautical Society Guidance and Control Conference, Breckenridge, CO, 2003, paper AAS 03-066.
³D. White, J. H. Schilling, S. Bushman, G. G. Spanjers, D. R. Bromaghim, J. Lake, and M. Dulligan, 33rd Plasmadynamics and Lasers Conference, Maui, HI, 2002, Paper AIAA 2002-2120.
⁴S. Orioux, C. Rossi, and D. Esteve, *Rev. Sci. Instrum.* **73**, 2694 (2002).
⁵S. Marcuccio, A. Genovese, and M. Andrenucci, *J. Propul. Power* **14**, 774 (1998).

- ⁶M. Gamero-Castaño and V. Hruby, *J. Propul. Power* **17**, 977 (2001).
⁷K. W. Stark, T. Dennis, D. McHugh, and T. Williams, AIAA 8th Electric Propulsion Conference, Stanford, CA, 1970, Paper AIAA 70-1111.
⁸A. J. Jamison, A. D. Ketsdever, and E. P. Muntz, *Rev. Sci. Instrum.* **73**, 3629 (2002).
⁹M. Gamero-Castaño, V. Hruby, and M. Martínez-Sánchez, 27th International Electric Propulsion Conference, Pasadena, CA, 2001, Paper IEPC-01-235.
¹⁰J. K. Ziemer, 27th International Electric Propulsion Conference, Pasadena, CA, 2001, Paper IEPC-01-238.
¹¹M. Gamero-Castaño and V. Hruby, 27th International Electric Propulsion Conference, Pasadena, CA, 2001, Paper IEPC-01-282.
¹²P. G. Maghami, F. L. Markley, M. B. Houghton, and C. J. Dennehy, American Astronautical Society Guidance and Control Conference, Breckenridge, CO, 2003, Paper AAS 03-065.
¹³M. Gamero-Castaño, *J. Propul. Power* (submitted).
¹⁴The development of this microPPT is an ongoing collaboration between the U.S. Air Force Research Laboratory and Busek. L. Byrne is responsible for the research work at Busek. D. Bromaghim is the manager of the program at the AFRL.